Project 2240 | July 2023

SJSU SAN JOSÉ STATE UNIVERSITY

MTI MINETA TRANSPORTATION INSTITUTE

Electrical Vehicle Charging Infrastructure Design and Operations

Yu Yang, PhD
Hen-Geul Yeh, PhD

CSUTC California State University Transportation Consortium

CALIFORNIA STATE UNIVERSITY LONG BEACH

Mineta Transportation Institute

Founded in 1991, the Mineta Transportation Institute (MTI), an organized research and training unit in partnership with the Lucas College and Graduate School of Business at San José State University (SJSU), increases mobility for all by improving the safety, efficiency, accessibility, and convenience of our nation's transportation system. Through research, education, workforce development, and technology transfer, we help create a connected world. MTI leads the Mineta Consortium for Transportation Mobility (MCTM) funded by the U.S. Department of Transportation and the California State University Transportation Consortium (CSUTC) funded by the State of California through Senate Bill 1. MTI focuses on three primary responsibilities:

Research

MTI conducts multi-disciplinary research focused on surface transportation that contributes to effective decision making. Research areas include: active transportation; planning and policy; security and counterterrorism; sustainable transportation and land use; transit and passenger rail; transportation engineering; transportation finance; transportation technology; and workforce and labor. MTI research publications undergo expert peer review to ensure the quality of the research.

Education and Workforce

To ensure the efficient movement of people and products, we must prepare a new cohort of transportation professionals who are ready to lead a more diverse, inclusive, and equitable transportation industry. To help achieve this, MTI sponsors a suite of workforce development and education opportunities. The Institute supports educational programs offered by the Lucas Graduate School of Business: a Master of Science in Transportation Management, plus graduate certificates that include High-Speed and Intercity Rail Management and Transportation Security Management. These flexible programs offer live online classes so that working transportation professionals can pursue an advanced degree regardless of their location.

Information and Technology Transfer

MTI utilizes a diverse array of dissemination methods and media to ensure research results reach those responsible for managing change. These methods include publication, seminars, workshops, websites, social media, webinars, and other technology transfer mechanisms. Additionally, MTI promotes the availability of completed research to professional organizations and works to integrate the research findings into the graduate education program. MTI's extensive collection of transportation-related publications is integrated into San José State University's world-class Martin Luther King, Jr. Library.

Report 23-14

Electrical Vehicle Charging Infrastructure Design and Operations

Yu Yang, PhD

Hen-Geul Yeh, PhD

July 2023

A publication of the
Mineta Transportation Institute
Created by Congress in 1991

College of Business
San José State University
San José, CA 95192–0219

TECHNICAL REPORT DOCUMENTATION PAGE

1. Report No. 23-14	2. Government Accession No.	3. Recipient's Catalog No.
4. Title and Subtitle Electrical Vehicle Charging Infrastructure Design and Operations		5. Report Date July 2023
		6. Performing Organization Code
7. Authors Yu Yang, PhD Hen-Geul Yeh, PhD		8. Performing Organization Report CA-MTI-2240
9. Performing Organization Name and Address Mineta Transportation Institute College of Business San José State University San José, CA 95192–0219		10. Work Unit No.
		11. Contract or Grant No. ZSB12017-SJAUX
12. Sponsoring Agency Name and Address State of California SB1 2017/2018 Trustees of the California State University Sponsored Programs Administration 401 Golden Shore, 5th Floor, Long Beach, CA 90802		13. Type of Report and Period Covered
		14. Sponsoring Agency Code
15. Supplemental Notes		

16. Abstract

California aims to achieve five million zero-emission vehicles (ZEVs) on the road by 2030 and 250,000 electrical vehicle (EV) charging stations by 2025. To reduce barriers in this process, the research team developed a simulation-based system for EV charging infrastructure design and operations. The increasing power demand due to the growing EV market requires advanced charging infrastructures and operating strategies. This study will deliver two modules in charging station design and operations, including a vehicle charging schedule and an infrastructure planning module for the solar-powered charging station. The objectives are to increase customers' satisfaction, reduce the power grid burden, and maximize the profitability of charging stations using state-of-the-art global optimization techniques, machine-learning-based solar power prediction, and model predictive control (MPC). The proposed research has broad societal impacts and significant intellectual merits. First, it meets the demand for green transportation by increasing the number of EV users and reducing the transportation sector's impacts on climate change. Second, an optimal scheduling tool enables fast charging of EVs and thus improves the mobility of passengers. Third, the designed planning tools enable an optimal design of charging stations equipped with a solar panel and battery energy storage system (BESS) to benefit nationwide transportation system development.

17. Key Words Operation research, System design, Predictive models, Heuristic methods, Electric vehicle charging	18. Distribution Statement No restrictions. This document is available to the public through The National Technical Information Service, Springfield, VA 22161.		
19. Security Classif. (of this report) Unclassified	20. Security Classif. (of this page) Unclassified	21. No. of Pages 52	22. Price

Form DOT F 1700.7 (8–72)

DOI: 10.31979/mti.2023.2240

Mineta Transportation Institute
College of Business
San José State University
San José, CA 95192–0219

Tel: (408) 924–7560
Fax: (408) 924–7565
Email: mineta-institute@sjsu.edu

transweb.sjsu.edu/research/2240

ACKNOWLEDGMENTS

The authors are grateful to the California State University, Long Beach (CSULB) Parking & Transportation Department for providing data. The authors also thank CSULB students Richard Nguyen, Nagarjun Chakka Sathyanarayana, and Nguyen Cam Thuy Dam for their work in collecting information. Finally, this project is financially supported by the Mineta Transportation Institute at San José State University.

CONTENTS

List of Figures

LIST OF TABLES

Executive Summary

As California becomes the pioneer state in promoting electric vehicles (EV) in the transportation sector, the incurred power demands of EVs may significantly lower the grid voltage and increase the travel expenses of EV users. Such drawbacks will degrade appliance function, lead to safety issues in the power grid, and worsen traffic congestion. In addition, private businesses can be hindered by these troubles and are reluctant to invest in the construction of new charging stations. The proposed project aims to achieve a satisfactory solution to recover the voltage drop induced by EVs charging through photovoltaic (PV) inverters, enable the most efficient charging scheduling, and minimize a charging station's operation cost through infrastructure optimization.

In this research, the team collects the charging demands and duration data from 2019 on the California State University, Long Beach campus and the solar power and weather data from the Long Beach Airport. The prices of charging service and batteries are from up-to-date market information. The time-of-use price of electricity for a 500 kW charging station is from the utility company Southern California Edison (SCE), with slight modifications. The gathered datasets are synthesized to create simulation scenarios for the charging schedule and station infrastructure optimization. The data sampling time and operation interval are both 15 minutes, which is long enough for a real-time calculation and scheduling. The software platform is GAMS with various state-of-the-art optimization solvers, such as SCIP, to ensure near-global optimality. Two scheduling algorithms, including robust model predictive control (MPC) and empirical rule-based methods, are proposed and compared under different scenarios and purposes. A response surface methodology (RSM) is further developed for the infrastructure optimization and handling the non-differentiable formula.

As the results of this work, the research team lists the following discoveries:

- Solar panels used in the charging station's power supply can reduce operational costs while making transportation greener.
- The proposed mathematical programming-based scheduling algorithm facilitates charging stations in meeting customers' demands in charging power and wait time. Without considering voltage recovery, this rule-based method is more efficient than the robust MPC in computational time and solution profitability.
- The RSM is better integrated with the rule-based approach for infrastructure optimization, whereas the robust MPC can be used for validation or policy improvement.
- The battery energy storage system may not be economically efficient under the current market price and net surplus compensation rate issued by the utility.

This project has led to one peer-reviewed journal publication: “A Robust Model Predictive Control-Based Scheduling Approach for Electric Vehicle Charging with Photovoltaic Systems,” Yu Yang, Hen-Geul Yeh, and Richard Nguyen, *IEEE Systems Journal*, Vol. 17, no. 1, 111–121, and another paper has been submitted to the journal, *IEEE Transactions on Transportation Electrification*.

1. Introduction

The U.S. government has invested $15 billion in the national network of 500,000 charging stations in the American Jobs Plan (The White House, 2021a). It also plans to reach 100 percent carbon-pollution-free electricity by 2035 and reduce carbon pollution from the transportation sector (The White House, 2021b). In California, both the California Energy Commission (CEC) and Caltrans have established several funding opportunities, such as the Electric Program Investment Charge (EPIC) program, to encourage innovative solutions for the deployment of electric vehicle (EV) infrastructure. A promising solution is to integrate EV charging stations with solar farms built on university campuses, shopping malls, and multifamily apartments to benefit a wide range of passengers. The proposed research will develop a simulation-based tool to design and operate such an integrated system more economically.

1.1 Project Background and Motivation

Multifamily apartment residents, long-distance commuters, and disadvantaged communities need a convenient, affordable, and reliable public charging network at Level 2 (AC-slow) or 3 (DC-fast) for their daily transportation. With limited space and budget, intermittent renewable sources, and grid restrictions, a solar-powered charging station must balance its investment, profitability, and utility. The proposed charging station design is shown in Figure 1. EVs can reserve the charging spots via vehicular communications, especially vehicle-to-vehicle (V2V) and vehicle-to-infrastructure (V2I) communications. Our scheduling algorithm will decide when and how to charge EVs through slow (Level 2) or fast chargers (Level 3). A solar farm will provide electricity to EV chargers during the daytime. If there is surplus electricity, then it will be sold to the grid. At night, either the grid or a battery will provide electricity to vehicles. We will design this green transportation system and develop its operational strategy to meet customer demand and maximize the operational profit of charging stations.

Figure 1. Solar Farm, Charging Station, And Communication Network

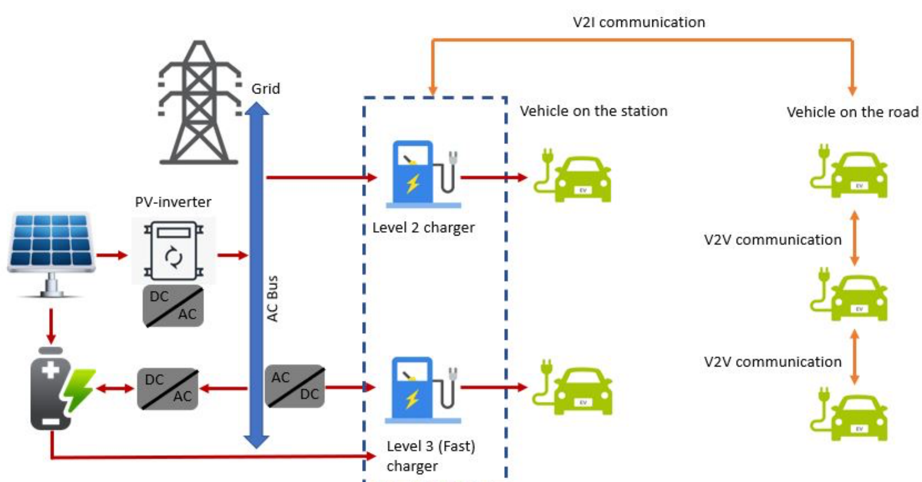

The related works on solar power prediction, EV charging management, and charging station design will be reviewed to identify any knowledge gaps and possible solutions.

Solar Power Prediction

The intermittent nature of solar power affects the renewable energy's supply to the charging station. Hence, a solar power prediction model is indispensable for schedulers to hedge the energy shortage. Solar power forecast approaches can be based on physical, statistical, and machine-learning models. The physical models use either previous observations or numerical weather predictions (NWPs) as inputs. For example, the total sky imager (TSI) model relies on image processing and cloud tracking for 15–30 minutes ahead of the prediction (Chow et al., 2011). Several types of clear sky models can be used to estimate solar irradiance (Antonanzas-Torres et al., 2019), which then serves as an input into a solar photovoltaic (PV) modeling algorithm for power generation predictions (Clack, 2017). The statistical approaches for short- and long-term forecasts based on autoregressive models have been extensively studied by Bacher et al. (2009). A probabilistic model has been developed by Loeper et al. (2020) to determine the joint distribution of hourly-ahead horizontal irradiation and measured solar power supply.

Many machine learning methods have been applied for solar power prediction and have shown significant improvements over the traditional physical and statistical approaches. Neural network (NN) models have been very popular as solar power predictors since the 1990s (Inman et al., 2013). Other machine learning methods, such as support vector machines (SVM) using multiple kernels (Sharma et al., 2011) and Naïve Bayes models (Bayindir et al., 2017), have been also applied in the literature. A comprehensive comparison study on the day-ahead hourly forecast of solar power generation has been presented in Gigoni et al. (2015), where second-order grey-box regression methods, NNs, quantile random forests (RF), k-Nearest Neighbors (kNNs), and support vector regressions (SVR) have been investigated. Their results show that these approaches have similar overall accuracy. An ensemble average is then proposed to synthesize all of their advantages to achieve the best performance under all weather conditions.

EV Charging Scheduling

Traditional EV-charging scheduling methods solely focus on the transportation system to balance the use of charging stations and minimize the waiting/charging time. The first step is to collect station utilization information and arrival/departure time to build a data-driven model. Then, different algorithms, such as simulated annealing (Bodet et al., 2012), dynamic programming (Delikaraoglou et al., 2013), multiservice queuing model (Said et al., 2013), and greedy primal-dual (Yudovina and Michailidis, 2015), can be employed to optimize the EV-charging schedule. Beyond the physical model, EV users' charging preferences and behavior are studied to predict charging choices and responses to the service (Daina et al., 2017; Will and Schuller, 2016).

A more advanced centralized or decentralized scheduling scheme is to plan the charging by taking both the transportation demands and the grid input-output balance into account. The simultaneous charging of many EVs through the grid may adversely impact the power distribution system (Pieltain et al., 2011). This issue occurs when solar power is insufficient to meet energy consumption. Schedulers thus need to coordinate the charging operations economically and safely to shave the peak. For example, demand response can be adopted to shift the charging requests from peak to off-peak times, thus obtaining more economic benefits (Fan, 2012). Atallah et al. (2018) compared centralized and decentralized approaches for supercharging scheduling. The centralized method collects the information and solves a large-scale optimization problem to reach the optimal charging schedule, but may not be scalable to many EVs charging simultaneously. A decentralized strategy allows the charging decisions to be made by each EV individually. However, such a strategy may incur an avalanche effect on the grid in power load increasing (Amjad et al., 2018). Moreover, the vehicular network should be sufficiently reliable to ensure real-time communication and management.

Existing research on EV charging scheduling has two limitations: modeling and computations. First, stochastic models (Delikaraoglou et al., 2013; Said, 2013; Yudovina and Michailidis, 2015; Kim et al., 2017; Wu et al., 2012; Pantos, 2012) for mobility behaviors and power supplies are widely used, but the accuracy and generality of such models is rarely discussed. Moreover, the probabilistic models are difficult to solve within a deterministic optimization scheme. Second, most simulations are conducted for relatively small-scale problems because the integer programming algorithms cannot be easily scaled up. The off-the-shelf solvers, such as CPLEX, may take several minutes to solve a medium-sized charging problem (Keskin and Çatay, 2016). However, computational demand becomes much more substantial when power grid operations, such as load shaving, are required in the charging strategy.

To overcome these limitations, the research team: (i) collects EV charging data and predicts PV energy generation using a support vector machine (SVM) model based on selected kernels, which can be embedded into a deterministic optimization solver (Nguyen et al., 2021); and (ii) develops and compares centralized optimization and empirical rule-based algorithms to determine the charging power assignment for each EV in real-time. The joint design of solar power model, charging pattern, and the scheduling algorithm will make the resulting solution unique, more practical, and optimal.

Infrastructure Design and Cost Analysis

Charging infrastructure based on renewable energy aims to meet the growing demands of EV charging without affecting the grid's stability, which means avoiding harmonics and voltage fluctuations. The economic and environmental benefits of PV-based charging stations in Los Angeles have been proven in literature (Tulpule et al., 2013). A solar-powered charging system should be designed with a proper converter, battery, and PV panels to avoid overly aggressive capital investment. For example, many researchers (such as Hussain et al., 2019; Ding et al., 2015;

and Sbordone et al., 2015) have pointed out the significance of the optimal battery size in a charging station. In Mouli et al. (2015), the authors designed the PV array and battery size simultaneously to match charging demands. The latest research trend is integrating short-term scheduling and system designs to achieve an overall optimal solution (Quddus et al., 2019), in which two-stage stochastic programming is solved to design the system. However, such work omits the system's nonlinearity, and its optimality is not guaranteed. The new contribution of this project is to integrate charging system operation and design within a two-stage decision framework and solve it through RSM

1.2 Project Methods

The project roadmap is shown in Figure 2. We will formulate an infrastructure design as a two-level problem including economic optimization (upper-level) and charging scheduling (lower-level). The solar predictions, charging request scenarios, and grid models will be developed and embedded into the scheduling algorithm. Both centralized and decentralized scheduling will be developed in parallel and compared in efficiency.

Data Preparation

The research team has secured real-time EV charging data from a charging station with PV panels at the CSULB campus and solar power generation data from the Long Beach Airport. The EV-charging data of the CSULB campus during 2019 with charging time (ranging from 5 minutes to 11 hours), power, and service fees, have also been obtained. Based on the data collected, we can simulate and predict charging demand and solar power supply at CSULB. The time-of-use (TOU) rate (i.e., cost) of electricity for charging stations under 500 kW can be found on the Southern California Edison (SCE) website.

Data-driven Modeling

The research team has used the machine learning package scikit-learn in Python and MATLAB to model the solar power generation profile given some weather input data. The investigated methodologies include support vector machines (SVM), random forests (RF), LightGBMs, and linear auto-regression models. The results show that the linear auto-regression model with embedded feature extraction/selection outperforms other machine learning approaches in its prediction accuracy. The charging request data will be used to form different scenarios in the simulation.

EV Charging Scheduling

Both centralized and decentralized strategies will be developed for EV charging scheduling. In the centralized algorithm, we will develop and solve a mixed-integer program (MIP) for scheduling. The objective is to minimize operational costs while satisfying customers' requirements. When a charging request is received, the solver will decide the power rate and power source (grid, solar panel, or battery) along a long control horizon. The charging requests gathered on the CSULB campus under different solar irradiation conditions will be used to test the scheduling algorithm. The entire simulation and optimization framework is executed in the GAMS platform with state-of-the-art solvers.

Infrastructure Design

Once all models are established, we will design the EV charging site, including the number of chargers, capacity of solar panels, and the size of energy storage, through RSM. The merit of RSM is that it can explore the relationship between input and response variables more efficiently via the design of experiments. The objective function of infrastructure design is to maximize profitability while meeting car usage demands and budget. The overall scheme will be formulated as a two-level optimization problem. The lower level is scenario-based charging scheduling, which will be solved using centralized or decentralized algorithms. The upper level optimizes the expected profit by determining the PV penetration, number of Level 2 chargers, and battery capacity. This two-level formula can accurately estimate the profitability of the real system, but is difficult to optimize through common solvers. The research team will use RSM to sample the design space and achieve a near-optimal solution.

Figure 2. Technical Developments Roadmap

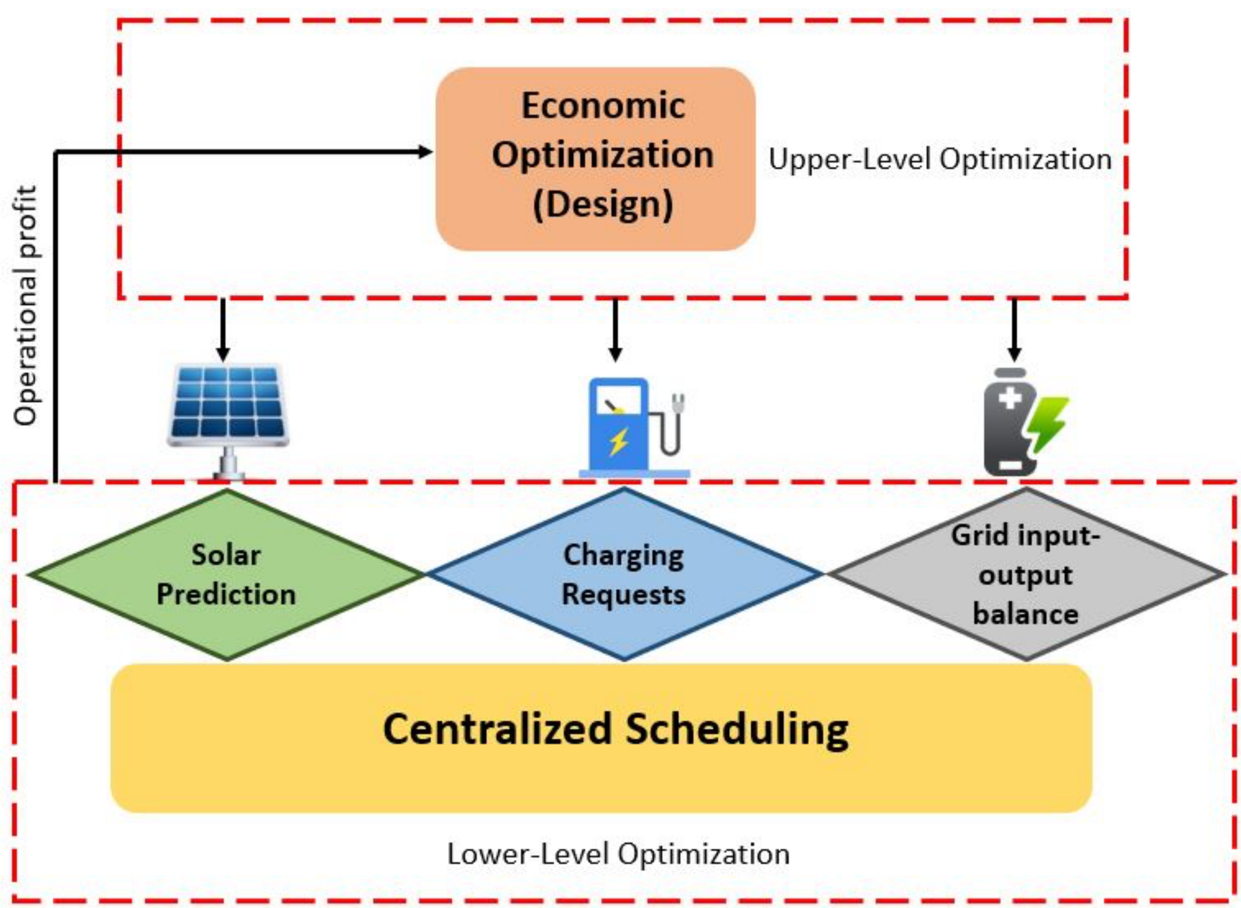

2. Robust Model Predictive Control for Electric Vehicle Charging

This section is based on the authors' paper: "A Robust Model Predictive Control-Based Scheduling Approach for Electric Vehicle Charging with Photovoltaic Systems," Yu Yang, Hen-Geul Yeh, and Richard Nguyen, *IEEE Systems Journal*, Vol. 17, no. 1, 111–121. A scheduling algorithm based on a robust MPC (R-MPC) is designed for the charging service at the CSULB campus parking lot with a solar power supply. The actual charging, solar generation, and weather data are gathered to build prediction models for EV charging demands and solar power supply. Then, these prediction models are embedded into mixed-integer nonlinear program (MINLP) formulas, which are solved in real time to determine optimal charging power. Different from Kabir et al. (2020), the proposed approach allows EVs to be charged either from the power grid or the solar energy system. Unlike Maigha and Crow (2017), this approach optimizes the profit of a charging station rather than the overall energy cost of the grid. Diverging from several studies (Kabir et al., 2020; Zhang et al., 2014; Li et al., 2020; Sun et al., 2020), the proposed approach does not assume any probabilistic model and makes a deterministic optimization formula instead. The proposed method has at least four advantages and novelties:

(i) The proposed approach allows the charging power to continuously vary rather than use constant current/voltage charging.

(ii) Only the proposed approach incorporates both PV power sales and TOU price into the optimization objective.

(iii) The one-step worst-case prediction is employed, and an additional optimization is solved to maximize the charging power without reducing profit. The resulting solution is more robust against uncertainties and avoids missing service.

(iv) Dynamic power load equations are used in our approach instead of the static one, leading to more accurate models .

2.1 Problem Formulation

A Modified IEEE-13 Node Test Feeder

The IEEE-13 node test feeder with a single-phase power supply is modified as a testbed, as shown in Figure 3. The following assumption is introduced:

Assumption 1. The charging station is on the leaf node of a power grid network.

Assumption 1 enables us to determine the voltage of a charging station without knowing the power load of other nodes. Accordingly, a charging station with a solar farm is constructed at node 652.

Node 650 is a substation with voltage V_{650} = 4.16 kV. The impedances under different configurations can be found in Kersting (1991). Two types of time-dependent power load models are employed in the simulation. One is for the general residential area, and the other is for large hotels. The active power loads generated by these models, denoted as p_j^c, are shown in Figure 4. The reactive power loads, denoted as q_j^c, are calculated by assuming the power factor to be 0.95.

The dynamics of real/reactive powers and voltage on a power grid can be described by the Distflow equations. In addition, the proposed scheme incorporates the maximum allowable reactive power generation from the IEEE-1547 standard. Since high charging demands render the node voltage below the limit, the reactive power injection at node 652 lifts the voltage and may recover from the instability (Turitsyn et al. 2015). Here, the voltage constraint at each node is set within the 1 ± 5% range.

Given power consumptions data at each node, the IEEE-13 node test feeder is simulated to generate dynamic voltage profiles. Then, voltage V_{684} will be fed into the R-MPC to renew power load constraints on p_j^c and q_j^c.

Figure 3. The Modified IEEE 13 Node Test Feeder

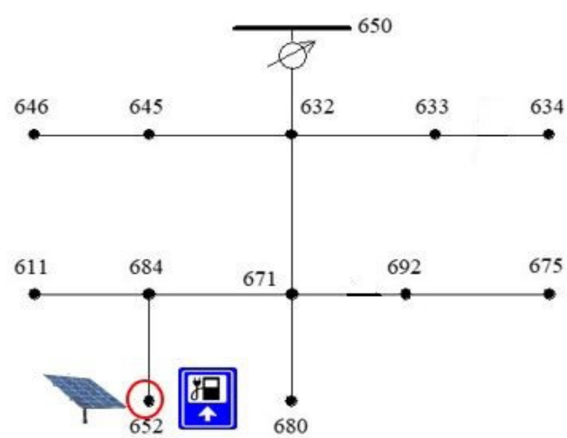

The Charging Station with Solar Panels is Introduced at Node 652

Figure 4. Left: Power Load for Three Residents

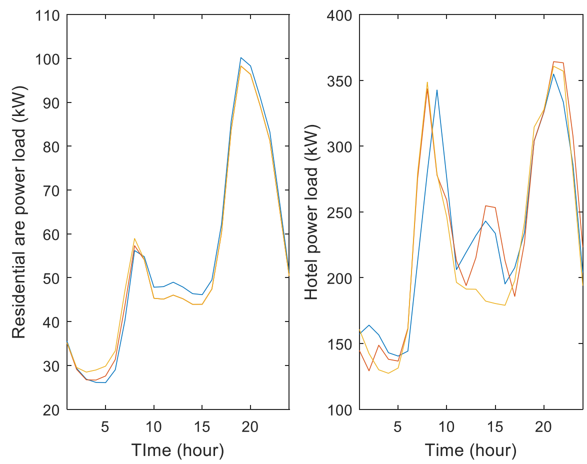

Right: Power load for three large-scale hotels.

Charging Station

The team selected a charging station on the CSULB campus with a PV power supply as the research target. In total, there are 44 SAE J1772 charging spots, each with a maximum power of 7.2 kW. A solar farm is built on-site with a maximum power generation S_{max} = 240 kW. The charging station primarily uses solar energy, and its power deficit is compensated by the grid. The TOU-EV-8 issued by SCE is applied. This tariff, denoted as $\alpha_B(h)$, is particular to EV charging stations whose monthly maximum demand is between 20 kW and 500 kW. Two profiles about $\alpha_B(h)$ are considered in the case studies:

Price I: 9:00 p.m. to 8:00 a.m.: $0.08 / kWh, 8:00 a.m. to 4:00 p.m.: $0.05 / kWh, 4:00 p.m. to 9:00 p.m.: $0.23 / kWh

Price II: 9:00 p.m. to 8:00 a.m.: $0.12 / kWh, 8:00 a.m. to 4:00 p.m.: $0.10 / kWh, 4:00 p.m. to 9:00 p.m.: $0.23 / kWh

The charging service fee is α_C = $0.40 / kWh at the CSULB campus. Apart from the charging service, the solar energy generated on-site can be sold back to the utility with α_S = $0.09 / kWh.

2.2 Schedule Design

In this section, a scheduling algorithm is designed to determine the charging power at each spot. The overall scheme is shown in Figure 5. A day is divided into 96 time slots with a sampling time interval of Δ = 0.25 hour. At each time instant, a scheduling problem is solved optimally to determine the charging power along a prediction horizon H. The objective of scheduling is to meet customer demands and maximize daily revenue. Inputs to the optimization-based scheduling tool include grid status, solar power generation, and charging demands. Note that a charging station node, denoted as s = 652, cannot know the power loads and flow on the entire power grid. Here the voltage at its parent node, denoted as ŝ = 684, is measurable in real time. However, voltage dynamics during the prediction horizon may not be known. Therefore, at any instant, the voltage prediction is a constant, $V_s(h|h) = V_{\hat{s}}(h + 1|h) = ... = V_{\hat{s}}(h + H|h)$, where (h + k|h) represents the prediction in k-step. Once the optimization algorithm calculates the charging power along the prediction horizon, denoted as C(h|h), C(h + 1|h),..., C(h + H |h), only C(h|h) is implemented. This scheme, the so-called receding horizon method, can adjust future operations based on real-time information. Repeating this process will generate an optimal charging profile for each EV.

Charging Demands Prediction

The charging data consists of the requested time, duration, and energy of each service event at the campus throughout the entirety of 2019. However, our scheduling algorithm only needs to forecast the number of charging requests at each decision time interval. Considering that customers, including university students and employees, may follow similar charging patterns during weekdays, historical data can be used to predict charging requests. The week-ahead average and maximum number of charging requests are denoted as $\tilde{\gamma}(h)$ and $\bar{\gamma}(h)$. Let $\hat{\gamma}(k + h|h)$ to represent the predicted number of incoming charging requests $\gamma(k + h)$ during time instant k + h. Then, the following prediction scheme is designed:

$$\hat{\gamma}(k + h|h) = \begin{cases} \bar{\gamma}(h + k)\ if\ k = 0 \\ \tilde{\gamma}(h + k)\ if\ 1 \leq k \leq H \end{cases}$$

Figure 5. The Overall Scheduling Schemes

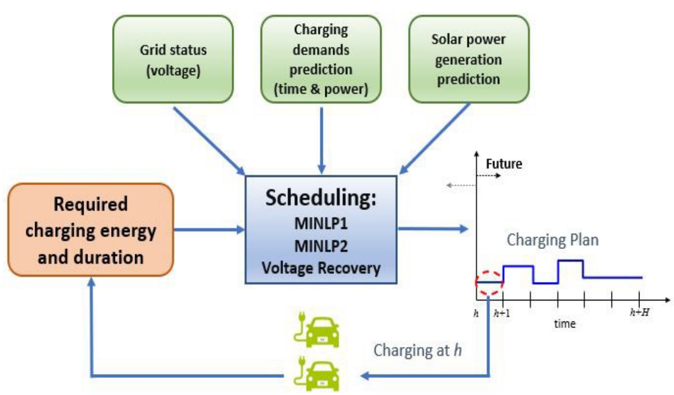

This is a one-step worst-case prediction, which impacts C(h|h) and ensures enough charging spots in the next 0.25 hours. Two designed datasets, shown in Figure 6, will evaluate the robustness of the scheduling algorithms. The busiest day (May 7) with 78 service requests is chosen as Test 1. It can be a good example to represent other untested real-world datasets. The second busiest day

(May 6) is modified by introducing additional charging requests with long durations. The resulting Test 2 has 107 service requests. Note that the required power of each EV may vary day by day and is difficult to forecast accurately. All predicted incoming EVs are assumed to be charged at the highest power rate of 7.2 kW. Figure 7 shows the aggregated energy demand at each time instant for the two tests. There are two peak hours of EV charging requests. One is around time instant 32 (8:00 a.m.) and another is around time instant 68 (5:00 p.m.). These two peak hours are directly related to the class schedule on campus. Morning classes start at 8:00 a.m. and evening classes start at 5:00 p.m. Only the total charging energy of each EV on the CSULB campus can be obtained, whereas the state of charge (SOC) information is not available. Thus, SOC is not considered in the proposed optimization algorithm.

Similarly, the allowed charging time for each incoming EV is not predicted because assuming the highest charging power already enables service to be completed earliest. The proposed algorithm has more flexibility to schedule the charging power for long-term tasks. Short-term tasks are more challenging because the time restriction forces the solver to charge that EV with high power.

Figure 6. Charging Requests in Every 0.25 Hours

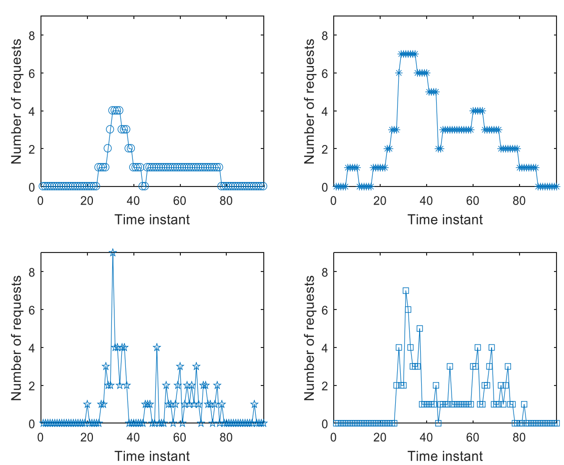

Left top: Week-ahead average.
Right top: Week-ahead maximum. Left bottom: Test 1 (May 7th). Right bottom: Test 2 (Synthetic).

Figure 7. Aggregated Energy Demands in Every 0.25 Hours

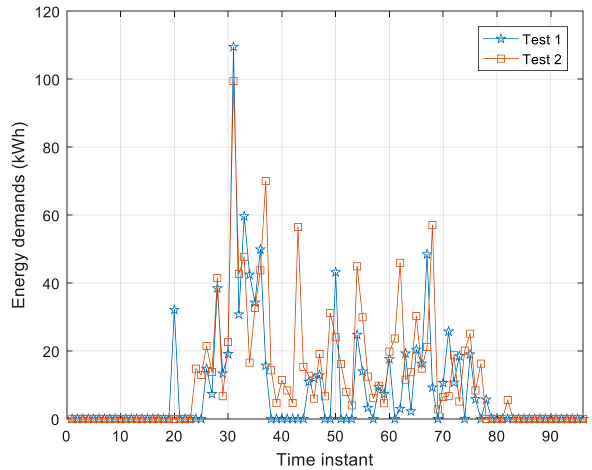

Solar Power Prediction

Solar power is a renewable but not reliable energy source to the EV charging system due to its weather-dependent and intermittent nature. An accurate prediction model for solar power generation is a critical component of the charging scheduling algorithm. Authors previously proposed a machine-learning approach to predict solar power using weather forecast (Yang et al., 2022). The dataset from the California Solar Initiative (CSI) used 15-minute interval power generation of a solar panel for training, validation, and testing. To make this paper self-contained, the machine-learning model is briefly introduced in this section.

The first step is to remove the mean from the training dataset, and the resulting power generation is denoted as $p^{g'}(h)$. The second step is to collect the weather input data and then build the model based on the autoregressive term, weather input, and time stamp. The regressor vector is defined as below:

$$\phi(h) = [p^{g'}(h-1), u_1(h), u_2(h), u_3(h), u_4(h), u_5(h), u_6(h), u_7(h)],$$

where $u_1(h)$ is the temperature; $u_2(h)$ is the dew point; $u_3(h)$ is the humidity; $u_4(h)$ is the wind speed; and $u_5(h)$ represents the time stamp. To represent the time-dependent nature of solar energy, two more variables are introduced: $u_6(k) = \cos(\pi u_5(k)/24)$ and $u_7(k)$ $\sin(\pi u_5(k)/24)$. The third step is feature construction. A simple linear regression model based on $\phi(h)$ has a limited capability for data fitting. Thus, $\phi(h)$ is normalized to build the first kind Chebyshev polynomial as a feature of the model. In addition, when there are clouds in the sky, one-hot encoding variables $u_9(h)$, $u_{10}(h)$, and $u_{11}(h)$ are introduced to describe partly cloudy, mostly cloudy, and cloudy weather, respectively.

The solar prediction model is a weighted sum of the augmented features:

$$p^{g'}(h) = \sum_{\phi_{w,j} \in \Psi_{[i]}} a_{[i],w,j} \phi_{w,j}(h)$$

where subscript $[i]$ indicates the weather type, either fair or cloudy; the model parameter $a_{[i],w,j}$ is identified by solving a constrained least squares problem on the training dataset; and $\Psi_{[i]}$is the set of active features for weather type i. In Yang et al. (2022), $\Psi_{[i]}$ is built via a feature selection and elimination algorithm on the validation dataset. Compared with other machine-learning algorithms, the proposed approach is simpler and more accurate.

The proposed model has a low mean squared error to predict solar power in southern California's coastal areas (Yang et al., 2022). Figure 8 illustrates the one-hour ahead prediction together with the actual power generation in the testing dataset. Because our model is based on the weather forecast, its accuracy may not be suitable for long-term prediction. Hence, for more than a one-hour ahead prediction, $p^{g'}(h)$ will be used instead. This solar power prediction model will be integrated into the charging scheduling algorithm shown in the next sub-section.

Figure 8. One-Day Solar Power Profiles in the Testing Dataset

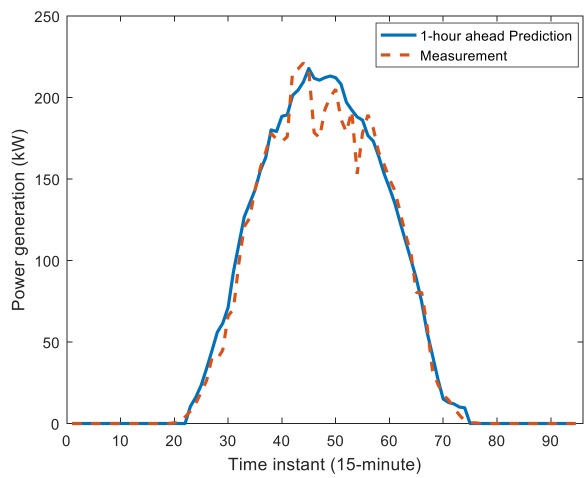

Scheduling Scheme

An R-MPC-based scheduling scheme is proposed by integrating optimization formulas with solar power predictions, charging requests predictions, and grid status. Each coming EV provides information on required energy and allowable charging time to the scheduler. Then, the scheduler solves a centralized optimization problem (MINLP1), shown in Figure 9.

Figure 9. Mixed-Integer Nonlinear Program 1 (MINLP1)

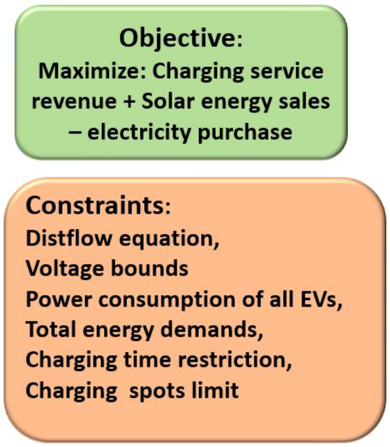

The formula shown in Figure 9 is a mixed-integer nonlinear program (MINLP), but can be simplified as an equivalent mixed-integer linear program (MILP). The number of binary variables is dependent on the quantity of charging EVs and the length of the prediction horizon H. When (MINLP1) is solved, there can be non-unique optimal solutions. For example, switching charging power at time instants h and h + 1 may obtain the same profit due to flat grid power price during the prediction horizon after sunset. Among these optimal solutions, the one with high $C_l(h|h)$ is preferred because it is less sensitive to the future prediction and is more likely to complete the charging service on time. To yield a more robust solution, the research team further proposes the following optimization formula (MINLP2):

Figure 10. Mixed-Integer Nonlinear Program 2 (MINLP2)

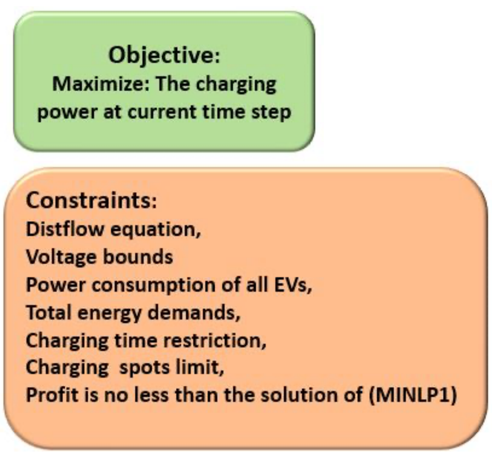

Voltage Recovery

In a receding horizon strategy, (MINLP1) and (MINLP2) are solved at a time instant h to determine $C_l(h+k|h), \forall k = 0,1,\dots,H$, whereas only $C_l(h|h)$ is implemented. However, because solar power generation, charging requests, and voltage predictions may not be accurate, the occurred scenarios can be different from the forecast. One of the issues is the overly low voltage when the power grid is subject to high power loads. Let us define a set $\Pi(h) \coloneqq \{l|7.2\Delta(T_l - 1) > \eta_l(h)\}$, such that $C_l(h|h), \forall l \in \Pi(h)$ does not delay the service. Here $\eta_l(h)$ represents the energy demand of charging spot *l* at time *h*. $T_l(h)$ is the allowable charging time of EV at spot *l* and time instant *h*. Then, the following algorithm adjusts the solution of $C_l(h|h)$ to satisfy the voltage constraint.

Algorithm 1:

Step 1 Implement $C_l(h|h)$ on the charging station.

Step 2 If $V_s < (1-5\%)V_{605}$, then go to Step 3; otherwise terminate Algorithm 1 and implement $C_l(h|h)$.

Step 3 Let $l^* = \arg min_{l\in\Pi(h)} \eta_l / T_l$.

Step 4 Let $C_{l^*}(h|h) = 0$, $\Pi(h) \leftarrow \Pi(h) \setminus l^*$, and go back to Step 1.

To quickly lift the voltage, Algorithm 1 repeatedly searches for the EV with the smallest average power and shuts down its charging service temporarily. As the resulting power load decreases, the voltage will rise.

2.3 Simulation Results

The IEEE-13 node test feeder is used to simulate a microgrid. Except the charging station node, power load profiles of other nodes in the grid have been shown in Figure 3. Two testing datasets are used to evaluate the proposed scheduling algorithm. The charging and PV power selling prices are constant, α_C = \$0.40 / kWh and α_S = \$0.09 / kWh. Two electricity purchase prices are simulated, shown in Subsection 2.1, to investigate the demand response. Price I encourages using grid power in EV charging, whereas Price II is favorable to the use of solar power. Two price profiles and two testing datasets result in four scenarios. The grid is simulated by using GAMS 32. To obtain the globally optimal solutions of (MINLP1) and (MINLP2), the solver SCIP (Achterberg, 2009) is used and terminated when the relative gap reaches 1%.

Four other charging schemes are implemented for comparison purposes. Here MPC-I, II, and III only change one feature of the proposed scheduling approach.

(i) Greedy charging: This strategy always uses the highest power to charge an EV whenever it arrives. If the total charging power on the station is overly high, then Algorithm 1 is used to recover the voltage drop.

(ii) MPC-I: Only the week-ahead average charging requests $\tilde{\gamma}$ is used for demand prediction.

(iii) MPC-II: Only (MINLP1) and Algorithm 1 are used to determine charging power.

(iv) MPC-III: Following Jiang and Zhen 2019, only three power levels—7.2 kW, 3.6 kW, and 0 kW—are provided for charging service.

Table 1 shows the operating profit, solution time, and missing service of considered approaches in four scenarios. Because our method takes both TOU price and surplus PV power sales into account, it yields a higher profit than the greedy method. Even though R-MPC has slightly less profit than MPC-II in scenarios 1, 3, and 4, it successfully completes all charging tasks, whereas MPC-II misses service in scenarios 2 and 3. Moreover, because our method employs a one-step worst-case prediction and maximizes the charging power through (MINLP2), it is more robust than all other MPC schemes. Another observation is that the discrete charging level in MPC-III reduces scheduling flexibility and introduces more binary variables into the optimization, resulting in less profit and longer computational time. The comparisons among these methods are shown in the following section.

Table 1. Profits ($)/Solving Time (Second)/Missing Service of Four Charging Methods

Methods	S1 Profit	S2 Profit	S3 Profit	S4 Profit
R-MPC	1579.4	1981.8	1561.4	1944.5
Greedy	1542.6	1910.8	1539.0	1906.8
MPC-I	1579.6	1953.8	1560.7	1944.9
MPC-II	1586.5	1975.2	1563.7	1945.3
MPC-III	1575.5	1891.0	1557.9	1932.1
	S1 Solving Time	S2 Solving Time	S3 Solving Time	S4 Solving Time
R-MPC	2.21	9.90	0.94	1.00
Greedy	0	0	0	0
MPC-I	1.63	2.87	0.36	0.78
MPC-II	0.86	4.17	0.35	0.68
MPC-III	220.98	694.05	103.88	151.28
	S1 Missing Service	S2 Missing Service	S3 Missing Service	S4 Missing Service
R-MPC	0	0	0	0
Greedy	0	0	0	0
MPC-I	0	2	0	0
MPC-II	0	2	3	0
MPC-III	0	9	0	0

Scenario 1: Test 1, Price I, Greedy MPC vs. R-MPC

Under Price I, the optimization-based scheduler prefers using grid power to charge EVs, and thus some charging tasks will be suspended until the accumulated power exceeds the solar power or allowable waiting time is used up. The charging profiles of the greedy method and R-MPC are shown in Figure 11. Their major difference occurs around time instants 30 to 42. Before time instant 32, R-MPC sells most solar power back to the grid and suspends non-urgent charging services. After h = 32, R-MPC generates several power peaks at h = 32, 37, 38, and 41 to meet time constraints or use more grid power. The greedy approach always maximizes the charging power and reaches its peak at h = 38. After time instant 64, the cost of electricity becomes much higher, and solar power decreases. The R-MPC arranges most of the charging work to time instant 84, when the grid power cost returns to a low level.

Figure 11. The Charging Profiles and Solar Power Generation (Scenario 1)

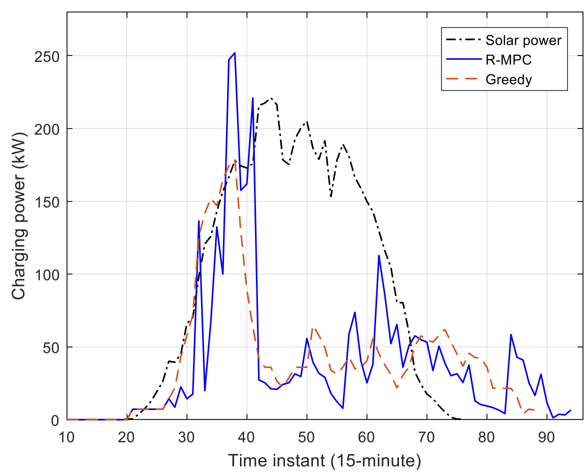

Scenario 2: Test 2, Price I, MPC III vs. R-MPC

MPC-III owns all R-MPC features but employs discrete charging levels. The resulting charging profiles are shown in Figure 12. Due to a large number of binary variables in its formula, MPC-III has a hard time reaching the optimal solution and does not sufficiently maximize the charging power between time instants 30 and 40. Therefore, the parking lot is full at time instants 42, 53, 61, and 62. The charging requests at those time instants have to be rejected.

Figure 12. The Charging Profiles and Solar Power Generation (Scenario 2)

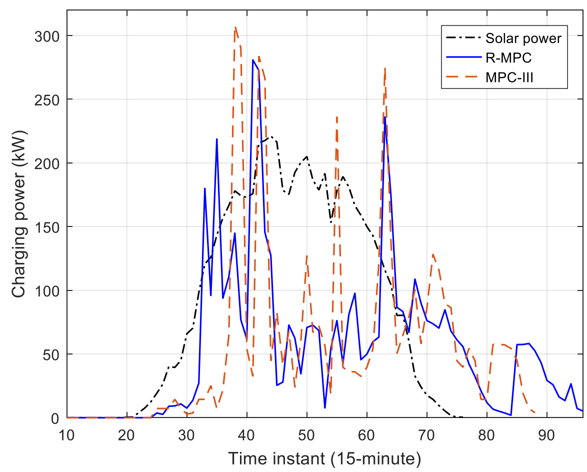

Scenario 3: Test 1, Price II, MPC II vs. R-MPC

Both R-MPC and MPC-II prefer using solar power to charge EVs under Price II. The resulting charging profiles are shown in Figure 13. Both schemes rely on optimization to determine the charging power. However, R-MPC further solves (MINLP2) to maximize the charging power such that all charging services can be completed on time. As a result, R-MPC generates 180 kW on time instant 37, whereas MPC-II only yields 50 kW at the same time step. Due to the high grid power load at time instant 82, shown in Figure 2, station voltage drops, and EV charging power is restricted. Because R-MPC has already completed most charging tasks, such an unpredicted voltage drop does not impact its charging time. On the contrary, MPC-II has more unfinished tasks at time instant 82, and thus lowering its charging power misses the service deadline.

Figure 13. The Charging Profiles and Solar Power Generation (Scenario 3)

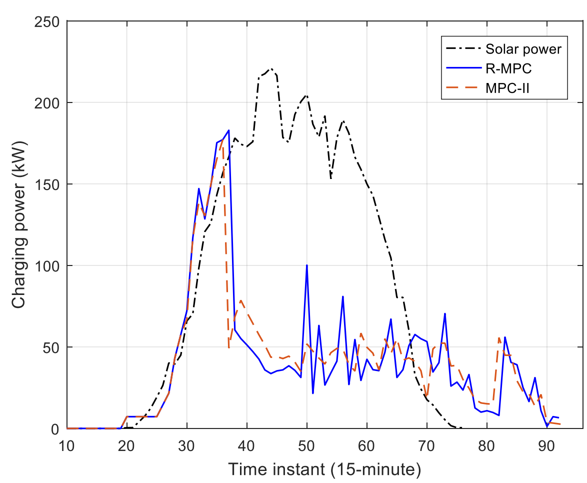

Scenario 4: Test 2, Price II, MPC I vs. R-MPC

The charging profiles of R-MPC and MPC-I are shown in Figure 14. They initially have the same charging power but diverge at time instants 36 and 37. The actual charging requests are $\gamma(36) = 3$ and $\gamma(37) = 5$. R-MPC employs the one-step worst case prediction $\bar{\gamma}(36) = 6$ and $\bar{\gamma}(37) = 6$, whereas MPC-I adopts the average prediction $\tilde{\gamma}(36) = 3$ and $\tilde{\gamma}(37) = 3$. Therefore, R-MPC yields higher power at h = 36 and h = 37 to complete existing tasks earlier such that more charging space can be vacated.

Figure 14. The Charging Profiles and Solar Power Generation (Scenario 4)

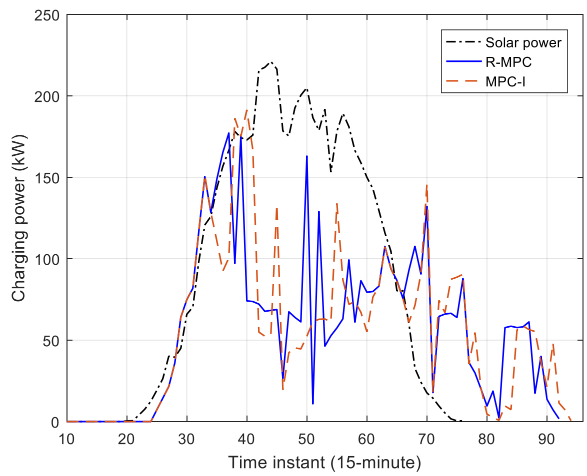

Finally, Figure 15 shows the voltage profile of all four scenarios using the proposed R-MPC and voltage recovery algorithm. The low voltage, near 0.95 p.u., happens between time instants 80 and 90, when high power loads are introduced at different nodes. Moreover, a small charging peak can be found during that period because several charging tasks are due before time instant 90. R-MPC always maximizes charging power at each time instant without reducing the profit, and thus it has more margin to lower its charging power during the peak hour.

Figure 15. The Voltage Under Four Scenarios Based On R-MPC

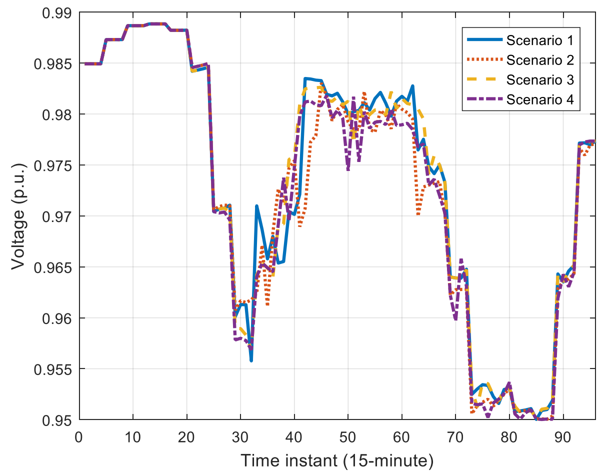

The lower limit is 0.95 p.u.

3. Sizing of Chargers, Solar Panels, and Batteries in the Design of EV Charging Stations

This section is based on the paper submitted to the *IEEE Transactions on Transportation Electrification* in December 2022. In this section, an optimization-based sizing method coupled with charging policy design is proposed based on the data collected from an EV parking lot at the CSULB campus. This information, including charging energy demands, allowable waiting time, as well as solar power generation, is analyzed to develop different charging policies, such as model prediction control (MPC) and empirical rule under a certain infrastructure setting. MPC assumes that one-hour ahead solar power can be known accurately. Then, the operational revenue of a charging station is maximized repeatedly by optimizing the charging power of each EV through a receding horizon manner while the time-of-use (TOU) price and the battery storage energy system's (BESS) charging/discharging are taken into account. An empirical rule is also proposed without using any forecast. Note that a charging demand peak happens after 4 p.m. due to class schedules, when solar power is insufficient, and grid power price is high. The battery that is charged during the daytime by solar power can discharge after 4 p.m. to avoid using grid power. Charging priority is determined by the required energy and allowable waiting time. Given the MPC or empirical rule, we can efficiently enumerate different design combinations to obtain their resulting yearly operational revenue. Finally, the 10-year total profit is calculated by counting operational revenue and infrastructure investment together to choose the optimal sizing of PV capacity, the number of chargers, and BESS capacity.

Compared with existing works, our contributions are listed below:

(i) A two-stage decision process is proposed with the first stage consisting of size sampling and the second stage of charging policy design.

(ii) An MPC and an empirical rule are developed for EV charging schedules and compared. The team demonstrates that a well-designed empirical charging strategy is comparable with the MPC.

(iii) A response surface methodology (RSM) scheme is employed to solve the non-differentiable optimization problem for the sizing of charger numbers, BESS capacity, and solar panel capacity.

3.1 Problem Formulation

A charging station at the CSULB campus with a PV power supply is studied. The number of N SAE J1772 type-I chargers are installed, each with maximum power 7.2 kW. A solar farm is built on-site with a power capacity denoted as P. A BESS is acquired with a usable energy capacity denoted as B. The price of BESS with different capacities is denoted as α_B and is shown in Table 2.

The charging station primarily uses solar energy and its battery, with its power deficit being compensated by the grid. The TOU-EV-8 issued by the utility service provider SCE is applied. This tariff, denoted as α_G is particular to an EV charging station whose monthly maximum power demand is between 20 kW and 500 kW, as shown in Table 3.

Table 2. Battery Price for Various Capacities

12 kWh	16 kWh	20 kWh	24 kWh	28 kWh	32 kWh
$ 7,085	$ 9,185	$ 11,285	$ 13,385	$ 15,485	$ 17,580
36 kWh	40 kWh	44 kWh	48 kWh	52 kWh	
$ 20,470	$ 22,570	$ 24,670	$ 26,770	$ 28,865	

Table 3. Grid Electricity Price

Time	Oct.–May	Jun.–Sep.
8 a.m.–4 p.m.	0.10 $/kWh	0.12 $/kWh
4 p.m.–9 p.m.	0.23 $/kWh	0.28 $/kWh
9 p.m.–8 a.m.	0.12 $/kWh	0.12 $/kWh

The dataset from the California Solar Initiative (CSI) 15-minute interval power generation at Long Beach Airport is used to determine the solar energy profile. The commercial PV capacity factor in southern California is assumed to be 19.1%. The resulting solar power baseline has a similar shape as Figure 8. In addition, the charging data consisting of the requested time, duration, and energy of each service event on the CSULB campus during the entire year of 2019 is gathered for the simulation of the entire annual operation.

3.2 Solution Method

In this section, two charging strategies are developed by assuming the fixed values of N, B, and P. Once the most effective charging strategy is determined, the response surface methodology will be applied in Stage-I to optimize the infrastructure parameters of N, B, and P. It is worthwhile to note that the RSM-based design follows a reverse sequence (Stage-II first) to optimize the objective function and determine decision variables.

For the charging strategy design, the decision sampling time Δ is specified as 15 minutes, which is the same as the solar power measurement time interval. To be precise, the charging requests are aggregated within a 15-minute interval. Then, the charging power for each EV is determined and renewed every 15 minutes. When an EV arrives at the station, its required energy and allowed charging time will be notified to the operator. The research team assumes that each EV will leave the charging spot once the allowed waiting time is reached or the energy demand has been met. If all charging spots are occupied, then incoming charging requests will be ignored.

Model Predictive Control based Charging

MPC-based charging has been introduced in Section 3. Here, the BESS is further added into the formula. The research team found that the accurate prediction of future charging demands is a challenging task, and thereby only the on-spot EVs are considered in the MPC. It is also assumed that the voltage fluctuation can be compensated by the utility rather the charging station. The resulting MPC formula is solved at time instant h to maximize the H-step predicted revenue without considering the depreciation of materials at the charging station. Figure 16 shows the proposed scheme.

Figure 16. Mixed-Integer Nonlinear Program 3 (MINLP3)

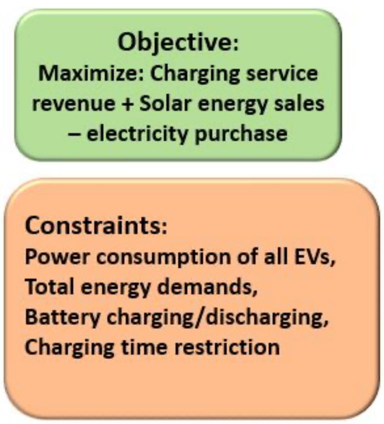

Figure 17. Mixed-Integer Nonlinear Program 4 (MINLP4)

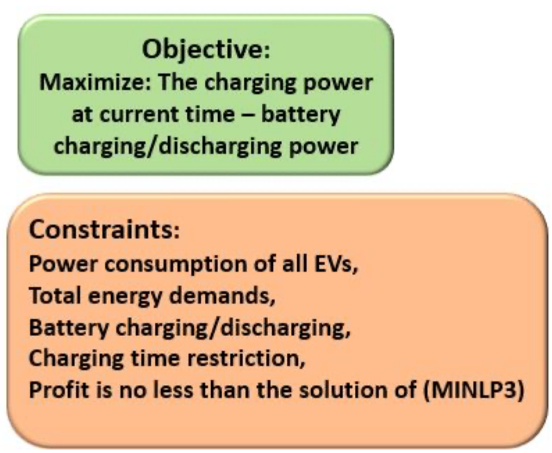

The discussions of MPC are presented in order. The objective function consists of three parts: charging fees, solar power sales to the grid, and power purchases from the grid. The battery's stored energy cannot exceed its capacity. When the allowable charging time is shorter than the prediction horizon, MPC requires the charging to be finished on time. When the allowed charging time is longer than the prediction horizon, then the charging profile is determined by assuming a maximum power of 7.2 kW can be used out of the prediction horizon. The battery charging and discharging rate $b(h)$ is limited as 0.2 C-rate. Namely, the full charging or discharging time is 5 hours. Ideally, a long prediction horizon in the MPC is preferred. However, solar power's long-term forecast error and its increased computational demand prohibit us from further increasing H.

After solving MINLP3, the charging power at the current time instant should be maximized because the incoming charging requests are not considered. The proposed MINLP4 is similar to MINLP2, but further minimizes battery charging/discharging fluctuations, as shown in Figure 17. Through this formula, the resulting charging policy will enable a parking lot to complete existing services earlier and accept more requests.

Mathematical programs (MIMLP3) and (MINLP4) should be solved every 15 minutes with updated solar power and charging requests data to design the charging profiles for each on-spot EV. The incurred revenue at each time step is accumulated to obtain the true operational revenue R. Infrastructure parameters B and P explicitly impact the solution of MPC. Even though the number of charging spots N is not shown in (MINLP3) and (MINLP4), it determines whether incoming EVs can be accepted or not. The program's complexity depends on the number of charging cars and resulting binary variables. The solution quality of MPC relies on the prediction accuracy of solar power generation which may be subject to substantial fluctuations. This drawback motivates us to develop a prediction-free scheme of the charging strategy.

An Empirical Rule Method

An empirical rule method is proposed in this subsection to schedule EV charging without using any prediction. First, note that the BESS can be charged using solar power without incurring any operational cost. When the grid power price becomes high, the BESS can provide power for EV charging to reduce the energy usage from the grid. Therefore, the rules of battery charging and discharging are:

- The charging process of BESS starts from 6:00 a.m. and should be completed before 4:00 p.m., denoted as TB.
- After 4:00 p.m., the battery is used for EV charging with higher priority due to the rising price of grid power.
- The energy in the BESS will never be sold to the grid.

The BESS charging period is determined based on the sunrise time and TOU price. Because α_G is much higher after 4:00 p.m., it is more profitable to use battery-stored power. Similarly, because α_C is much higher than α_S, all BESS power will be stored for charging service rather than selling to the grid.

At time instant h, the minimal charging power of an EV at spot l, denoted as $\underline{x}_l$ or battery $\underline{b}$, is defined as:

$$\underline{x}_l(h) = min\left\{7.2, max\left\{\frac{\eta_l(h)}{\Delta} - 7.2(T_l(h) - 1), 0\right\}\right\}$$

$$\underline{b}(h) = min\left\{0.2B, max\left\{\frac{\beta(h)}{\Delta} - 0.2B(T_B(h) - 1), 0\right\}\right\}$$

where $\beta(h)$ is the available energy of battery at time instant h. From 6:00 a.m. to 2:00 p.m. on a weekday or 6:00 a.m. to 4:00 p.m. on weekends, the minimal power is supplied first through the PV, and the gap can be compensated by the grid. If extra solar energy is available, it should either be stored in the battery or used to charge EVs before anything else. If no EV or BESS needs power, then the surplus solar power can be sold back to the grid.

- On weekdays between 6:00 a.m. and 2:00 p.m. or weekends between 6:00 a.m. and 4:00 p.m., the charging power is initialized as its minimal value $\underline{x}_l(h)$ or $\underline{b}(h)$.

- If $p^g(h) > \sum_{l\in\Theta(h)} x_l(h) + b(h)$, then select an EV labeled as l^* with the shortest allowable waiting time, denoted as $T_{l^*}(h)$, whose charging power is

$$x_{l^*}(h) = max\left\{min\left\{7.2, p^g(h) - \sum_{l\neq l^*} \underline{x}_l(h) - b(h), \eta_{l^*}(h)/\Delta\right\}, \underline{x}_l(h)\right\}$$

- If BESS has the shortest allowable charging time and extra solar power is available, then there is

$$b(h) = max\left\{min\left\{0.2B, p^g(h) - \sum_{l\neq l^*} \underline{x}_l(h), \beta(h)/\Delta\right\}, \underline{x}_l(h)\right\}$$

Repeat the above process to enumerate EVs and the BESS until the solar power is used up. Here, the $\eta_{l^*}(h)/\Delta$ or $\beta(h)/\Delta$ is embedded into the calculation to avoid overcharging. The charging load is initialized by the minimal required power and gradually increased to a full use of solar power.

To avoid peak time charging on weekdays, the EVs should obtain as much energy as possible before 4 p.m. In addition, it is unnecessary to delay the charging load after 2:00 p.m. when solar energy generation starts decreasing. The resulting rule is

- On weekdays between 2:00 p.m. and 4:00 p.m., the charging power of EVs at spot l is

$$x_l(h) = min\{7.2, \eta_l(h)/\Delta min\{T_l(h), 65 - h\}\}$$

$$b(h) = min\{0.2B, \beta(h)/\Delta(65 - h)\}$$

The above rule for $x_l(h)$ or $b(h)$ aims to complete charging service before 4 p.m., subject to a maximum power of 7.2 kW or 0.2 B.

During peak hours, charging tasks should be kept at a minimum in order to shift the load to the off-peak time. In addition, non-grid power, including solar and battery power, is denoted as $p^{g\prime}(h) = p^g(h) + min\{0.2B, \beta(h)/\Delta\}$.

- Between 4:00 p.m. and 9:00 p.m., the charging power is initialized as its minimal value $\underline{x}_l(h)$.

- If $p^{g\prime}(h) > \sum_{l\in\Theta(h)} x_l(h)$, then select an EV labeled as l^* with the shortest allowable charging time, denoted as $T_{l^*}(h)$, whose charging power is

$$x_{l^*}(h) = max\left\{min\left\{7.2, p^{g\prime}(h) - \sum_{l\neq l^*} \underline{x}_l(h), \eta_{l^*}(h)/\Delta\right\}, \underline{x}_{l^*}(h)\right\}$$

Repeat the above process until battery energy is used up or no charging is needed.

- The battery discharge rate is

$$b(h) = -min\left\{\frac{\beta(h)}{\Delta}, 0.2B, max\left\{\sum_{l\in\Theta(h)} x_l(h) - p^g(h), 0\right\}\right\}$$

At night, the charging power can be evenly distributed to each time instant due to flat grid electricity price $\alpha_G(h)$. However, if the desired departure time is later than sunrise, such tasks can be delayed in order to use solar energy. Let T_l' denote the allowed charging time period after 6:00 p.m. If the departure time of an EV at spot l is before 6:00 p.m., then $T_l' = 0$.

- Between 9:00 p.m. and 6:00 a.m., the charging power of an EV at spot l is

$$x_l(h) = min\left\{7.2, max\left\{0, \frac{\eta_l(h) - 7.2\Delta T_l'}{\Delta min\{T_l(h), T_{h\to 6}\}}\right\}\right\}$$

where $T_{h\to 6}$ denotes the period from the current time instant to 6:00 a.m.

- Battery discharging between 9:00 p.m. and 6:00 a.m. is

$$b(h) = -min\left\{0.2B, \frac{\beta(h)}{\Delta}, \sum_{l \in \Theta(h)} x_l(h)\right\}$$

Compared with MPC, the empirical rule approach does not rely on any predictor and optimization solver. Hence, it is more robust and quicker to make the charging decision. It is worthwhile to note that the pattern of solar power generation in southern California is relatively steady, and the daily charging peak time at our campus does not vary considerably due to the class schedule. The proposed charging strategy is thus implementable.

Response Surface Methodology to Optimize Infrastructure

In this subsection, the RSM is applied to optimize the infrastructure, including PV capacity P, battery capacity B, and the number of charging spots N. How these parameters influence the total profit is not described in previous sections analytically. Note that MPC relies on the receding horizon method to determine and modify operations on-the-fly and thereby cannot be used for long-term economic optimization. The empirical rule does not even have an optimization formula. RSM is a suitable tool to build an empirical relationship between infrastructure parameters and total profit, equal to operational revenue minus capital investment, through data fitting. Then, such an empirical model can be used for overall economic optimization. The algorithm flowchart of RSM is shown in Figure 18.

The research team chooses the 3-factor BB design to explore the solution space, and thus only 13 solutions need to be evaluated at each iteration. Three levels for B, N, and P are denoted as L_B, L_N, and L_P, with possible values of -1, 0, and 1. The level distance depends on the variable range, denoted as λ_{B}, λ_N, and λ_P, respectively. As a result, the explored solution of BB design can be expressed as:

$$B = B^* + L_B\lambda_B, N = N^* + L_N\lambda_N, P = P^* + L_P\lambda_P$$

where B^*, N^*, P^* are the optimal solution in the previous iteration.

Figure 18. RSM Algorithm Flowchart

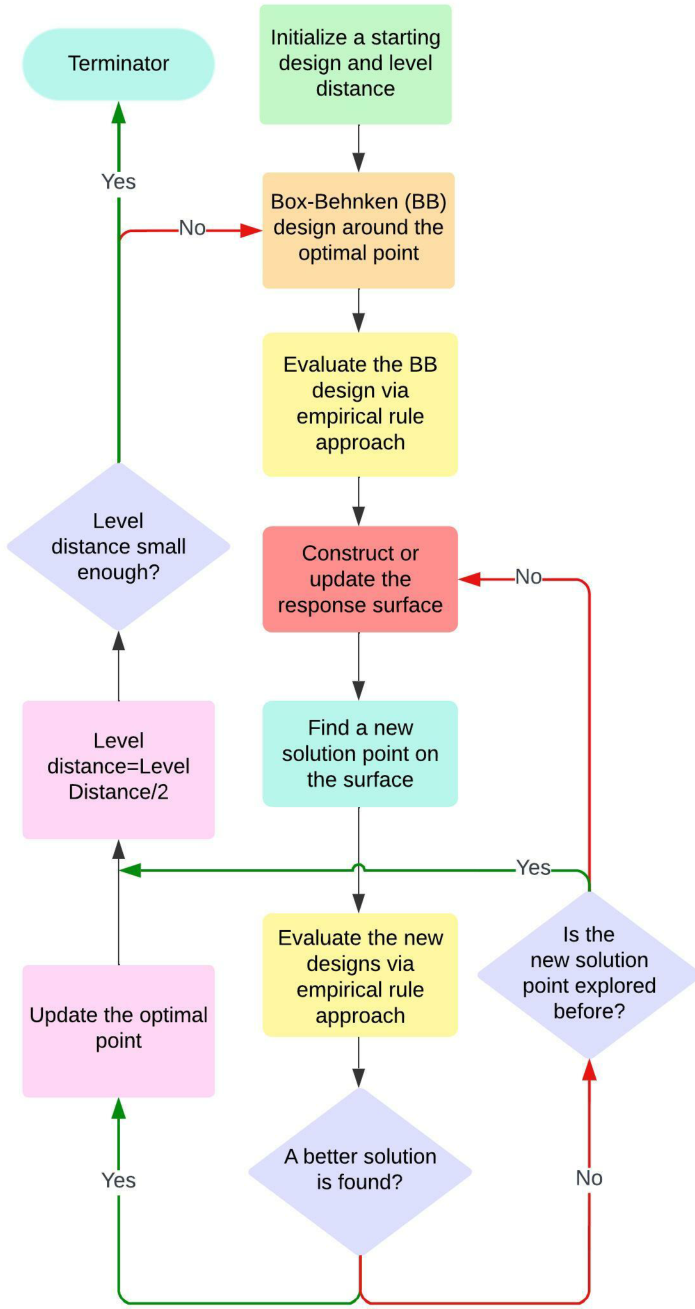

In the evaluation step, the yearly operational revenue, denoted as $\mathcal{R}$, is obtained via the empirical rule method instead of MPC to avoid the MPC-incurred high computational demand. The capital investment includes charger, BESS, and PV panel. The Level 2 charger equipment and installation fee in a public site is $6,000 per plug. The HVL battery price α_B for the U.S. market is shown in Table 1. The unit price of a commercial rooftop PV-panel is $1:56/$W_{DC}$ in the 2021 U.S. market, with a $17/kW maintenance cost per year (Ramasamy et al. 2021). Therefore, the 10-year total profit is:

$$\mathcal{H}(B, N, P) = 10\mathcal{R} - \alpha_B(B) - 6000N - (1560 + 170)P$$

Here we assume that the BESS, charger, and PV-panel have at least a 10-year lifespan without any capacity reduction.

Given the sampled factors and associated response, a quadratic surface function can be generated:

$$\widehat{\mathcal{H}}(B, N, P) = const + c_B B + c_N N + c_P P + c_{B2} B^2 + c_{N2} N^2 + c_{P2} P^2 + c_{BN} BN + c_{BP} BP + c_{PN} PN$$

where constants $C_{B,} C_{N,} C_{P,} C_{B2}, C_{N2}, C_{P2}, C_{BN}, C_{BP},$ and C_{PN} are model coefficients to be identified through factor-response data. Then, a new solution can be searched on the surface function. Note that B, N, and P are all integer variables, and thus the resulting optimization is a mixed-integer quadratic program (MIQP), which can be solved to its global maximum via commercial solvers. If such a solution is not better than existing ones, then the surface function $\widehat{\mathcal{H}}$ can be updated for continued searching. If that solution is better than others or has been evaluated in previous iterations, then level distance is deducted, and the BB-design is conducted again around the existing optimal solution. The RSM terminates when the searching space shrinks to a small value.

3.3 Simulation Study

In this section, only the empirical rule is used in the RSM for infrastructure design because of its fast calculation. Yearly, solar power and charging request data is used to obtain the annual operation revenue. Once the optimal values of B, P, and N are determined, MPC is evaluated and compared with the empirical rule method. The optimization platform is GAMS 41.2.0, with solvers CPLEX and SCIP (Achterberg, 2009). Both CPLEX and SCIP termination conditions are specified as reaching a 0.1% relative gap or 200 seconds of wall-clock time.

The initial feasible range of each design variable is shown below. However, if a better solution is found close to the boundary, then the searching area will be expanded.

$$B \in [12,52] \cup 0, N \in [14,44], P \in [100,240]$$

Table 4 shows the initial 13 sampled BB-designs and associated 10-year total profits. The analysis of variance (ANOVA), including F-value and p-value, is attached to quantify the influence of three design parameters to the total profit. Note that the p-value of each factor is small or even zero, which implies that all three variables have significant influence on the profit and thus should be considered simultaneously.

Table 4. Initial 13 Sampled Designs

H	*B*	*P*	*F*
195707.860	12	100	32
74361.710	12	240	32
186334.470	52	100	32
65927.510	52	240	32
185445.120	12	170	20
75197.460	12	170	44
175874.770	52	170	20
67100.760	52	170	44
226773.780	32	100	20
128145.940	32	100	44
119373.290	32	240	20
3004.400	32	240	44
140852.350	32	170	32
F-value	5.38	921.4	779.92
p-value	0.0459	0	0

Figure 19 shows the profit of the evaluated designs in the RSM. The initial 13 designs distribute into a large design space, and thus the resulting profit fluctuates substantially. Once the quadratic surface is constructed, a better solution is found at the 14th sample. As the level distance is reduced, the sampling space shrinks, and the profit curve becomes smoother. The RSM terminates when the level distances of *B* and *N* has reached 1. The optimal solution is found at the 52nd sample.

Figure 19. The Profit Evolution in RSM

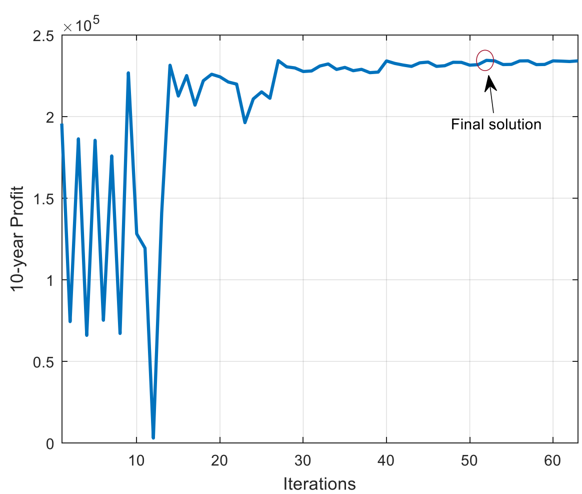

Figure 20 shows the 3-dimensional (3D) design space and the profit in color. The high-profit region has more samples to reach the near-optimal design. It clearly shows that large PV-panel or BESS capacity reduces the overall profit because high capital investment prolongs the payback period. The optimal solution is shown in Table 5. Even though BESS can shift some of the solar power to peak hours after sunset and thus generate more revenue, the solver still prefers not to use BESS due to its high cost. For comparison, we also show the solution with minimum BESS capacity (12 kWh), which is less profitable. The number of charging spots is also not large enough, such that some charging requests are declined when the station is full. Even though this may lose some revenue, the capital cost is saved.

Figure 20. The Evaluated Design and Associated 10-year Profit

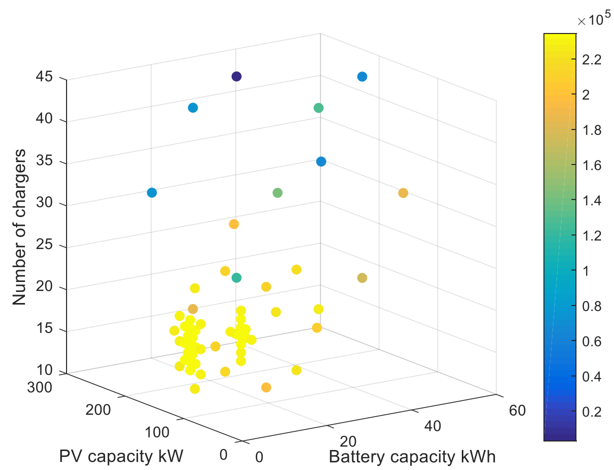

Besides the rule-based operation strategy, MPC with a prediction horizon $H = 15$ is executed to determine annual operations, given the sizing solution B, N, and P. The results are also shown in Table 5. It is not surprising to see that MPC takes a significantly longer time to compute the year-long operation because it needs to solve (MINLP3) and (MINLP4) for each time instant. Due to real time optimization, MPC slightly outperforms the rule-based method regarding operational revenue and declined services when the battery is not used. However, the long solution time prohibits its application in the RSM. Increasing the relative gap can shorten the computational time, but the solution's optimality cannot be guaranteed. In addition, when battery use is enforced, MPC needs to decide whether the battery or EV is charged based on the inaccurate prediction of solar power. This complexity makes the MPC take an even longer time and yield less revenue. On the contrary, the proposed rule-based method takes much less time because of its optimization-free nature and achieves similar results without using a solar power prediction. Hence, the rule-based method can be a more practical choice in RSM-based infrastructure sizing.

Table 5. Solution Profit, Time, and Declined Services

Optimum (B: 0, P: 84, N: 19)	Rule-based	MPC-based
P($)	234429.99	240914.55
Simulation Time (minutes)	9.8	772.5
Optimum w/ BESS (B: 12, P: 84, N: 19)	Rule-based	MPC-based
P($)	231855.86	213423.13
Simulation Time (minutes)	11.9	3539.7

Figure 21 shows the sampled daily EV charging profiles using rule-based and MPC-based strategies. The rule-based method charges EVs by following the solar power profile in order to save cost, whereas the MPC method allows much higher charging power in order to complete existing services earlier and accept more charging requests.

Figure 21. Charging profiles and Solar Power in a Sampled Day (B = 0, P = 84, N = 19)

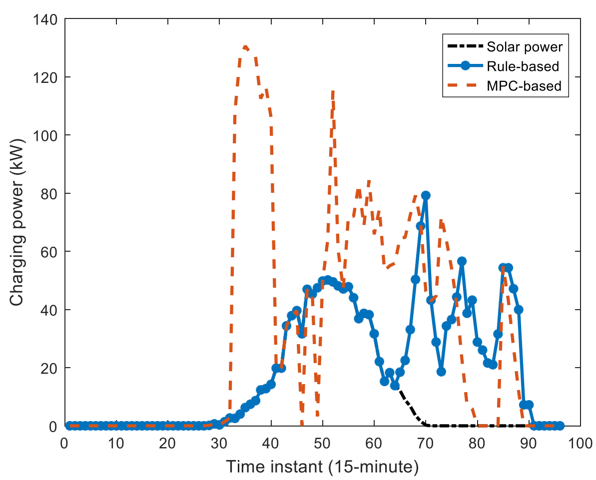

When a small-scale BESS (12 kWh) is deployed, the sampled daily battery charging/discharging profiles of MPC and rule-based approaches are shown in Figure 22. The rule-based method charges BESS before 4:00 p.m. and discharges it after 4:00 p.m. The MPC approach operates the BESS based on the optimization, which also charges the battery before 4:00 p.m. and discharges it at night. It is also worthwhile to note that the initial energy of BESS at that sampled day is non-zero because a year-long simulation is conducted.

Figure 22. Battery Charging/Discharging Profiles in a Sampled Day (B = 12, P = 84, N = 19)

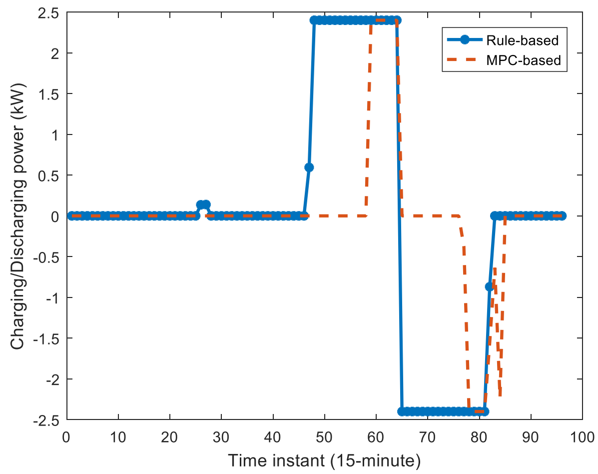

4. Summary & Conclusions

In this project, the research team designed electric vehicle charging policy and station infrastructure optimization algorithms. Two charging strategies, including MPC and empirical rule-based methods, are proposed and compared. The MPC is based on solar power prediction and needs to solve an optimization problem twice to determine the optimal solution while reducing the number of declined services. A voltage recovery approach can be applied with MPC to mitigate the prediction error on the voltage through reactive power injection. The empirical rule is designed heuristically and is prediction-free. Then, the RSM is developed to search the optimal design parameters, including PV capacity, battery capacity, and charger number, for 10-year profit maximization solely based on the empirical rule. One-year charging requests with solar power generation data collected on the CSULB campus are used to evaluate the proposed methodology. The simulation results show that the empirical rule approach yields similar revenue compared with the MPC, but requires a substantially shorter solving time and is thus particularly suitable to the RSM. The ANOVA result shows that PV capacity, battery size, and charging number are all important factors that impact the 10-year revenue of the charging station. The RSM-based optimal design demonstrates that the expensive BESS may not be necessary for the charging station if surplus solar power can be sold back to the grid. The proposed methodology can be applied to any EV charging station update if the solar power generation and charging requests data is available. In the future, the prediction-based empirical rule and battery capacity degradation can be two possible research directions to improve the current study.

Bibliography

Achterberg, T. “SCIP: solving constraint integer programs.” Math. Prog. Comp. 1, (2009): 1–41.

Amjad, M., Ahmad, A., Rehmani, M. H., and Umer, T. “A review of EVs charging: From the perspective of energy optimization, optimization approaches, and charging techniques.” Transportation Research Part D 62, (2018): 386–417.

Antonanzas-Torres, F., Urraca, R., Polo, J., Perpnan-Lamigueiro, O., and Escobar, R. “Clear sky solar irradiance models: A review of seventy models.” Renewable and Sustainable Energy Reviews 107, (2019): 374–387.

Atallah, R. F., Assi, C. M., Fawaz, W., Tushar, M., and Khabbaz, M. J. “Optimal supercharge scheduling of electric vehicles: Centralized versus decentralized methods.” IEEE Transactions on Vehicular Technology 67, (2018): 7896–7909.

Bacher, P., Madsen, H., and Nielsen, H. A. “Online short-term solar power forecasting.” Solar Energy 83, (2009): 1772–1783.

Bayindir, R., Yesilbudak, M., Colak, M., and Genc, N. “A novel application of Nave Bayes classifier in Photovoltaic energy prediction.” 16th IEEE International Conference on Machine Learning and Applications, 2017.

Bodet, C., Schulke, A., Erickson, K., and Jablonowski, R. “Optimization of charging infrastructure usage under varying traffic and capacity conditions.” Proc. IEEE 3rd Int. Conf. Smart Grid Communication, (2012): 424–429

Chow, C. W., Urquhart, B., Lave, M., Dominguez, A., Kleissl, J., Shields, J., and Washom, B. “Intra-hour forecasting with a total sky imager at the UC San Diego solar energy testbed.” Solar Energy 85, (2011): 2881–2893.

Clack, C. T. M. “Modeling solar irradiance and solar PV power output to create a resource assessment using linear multiple multivariate regression.” Journal of Applied Meteorology and Climatology 56, (2017): 109–125.

Daina, N., Sivakumar, A., and Polak, J. W. “Electric vehicle charging choices: Modelling and implications for smart charging services.” Transportation Research Part C 81, (2017): 36–56.

Delikaraoglou, S., Capion, K., Juul, N., and Boomsma, T. K. "Optimal charging of electric drive vehicles: A dynamic programming approach." Grid Integration of Electric Vehicles in Open Electricity Markets Chapter 5, (2013): 113–128.

Ding, H., Hu, Z., and Song, Y. "Value of the energy storage system in an electric bus fast charging station." Applied Energy 157, (2015): 630–639.

Fan, Z. "A distributed demand response algorithm and its application to PHEV charging in smart grids." IEEE Transactions on Smart Grid 3, (2012): 1280–1290.

Gigoni, L., Betti, A., Crisostomi, E., Franco, A., Tucci, M., Bizzarri F., and Mucci, D. "Day-ahead hourly forecasting of power generation from Photovoltaic plants." IEEE Transactions on Sustainable Energy 9, (2018): 831–842.

Hussain, A., Bui, V. H., Baek, J. W., and Kim, H. M. "Stationary energy storage system for fast EV charging stations: simultaneous sizing of battery and converter." Energies 12, (2019): 4516.

Inman, R. H., Pedro, H. T. C., and Coimbra, C. F. M. "Solar forecasting methods for renewable energy integration." Prog. Energy Combust. Sci. 39, no. 6 (2013): 535–576.

Jiang, W. and Zhen, Y. "A real-time EV charging scheduling for parking lots with PV system and energy store system." IEEE Access 7, (2019): 86184–86193.

Kabir, M. E., Assi, C., Tushar, M. H. K., and Yan, J. "Optimal scheduling of EV charging at a solar power-based charging station." IEEE Systems Journal 14, no. 3 (2020): 4221–4231.

Kersting, W. "Radial distribution test feeders." IEEE Trans. Power Syst. 6, 3 (1991), 975–985.

Keskin, M., and Çatay, B. "Partial recharge strategies for the electric vehicle routing problem with time windows." Transportation Research Part C 65, (2016): 111–127.

Kim, Y., Kwak, J., and Chong, S. "Dynamic Pricing, Scheduling, and Energy Management for Profit Maximization in PHEV Charging Stations." IEEE Transactions on Vehicular Technology 66, (2017): 1011–1026.

Li, H., Wan, Z., and He, H. "Constrained EV charging scheduling based on safe deep reinforcement learning," IEEE Transactions on Smart Grid 11, 3 (2020): 2427–2439.

Loeper, F., Schaumann, P., Langlard, M., Hess, R., Basmann, R., and Schmidt, V. "Probabilistic prediction of solar power supply to distribution networks, using forecasts of global horizontal irradiation." Solar Energy 203, (2020): 145–156.

Maigha, and Crow, C. L. “Cost-constrained dynamic optimal electric vehicle charging.” IEEE Transactions on Sustainable Energy 8, 2 (2017): 716–724.

Mouli, G.R.C., Bauer, P., and Zeman, M. “System design for a solar powered electric vehicle charging station for workplaces.” Applied Energy 168, (2015): 434–443.

Nguyen, R., Yang, Y., Tohmeh, A., and Yeh, H. G. “Predicting PV Power Generation using SVM Regression.” IEEE Green Energy and Smart Systems Conference (IGESSC), 2021.

Pantos, M. “Exploitation of electric-drive vehicles in electricity markets.” IEEE Transactions on Power Systems 27, (2012): 682–694.

Pieltain, F. L., Roman, T., Cossent, R., Domingo, C.M., and Frias, P. “Assessment of the impact of plug-in electric vehicles on distribution networks.” IEEE Transactions on Power Systems 26, (2011): 206–213.

Quddus, M. A., Kabli, M., and Marufuzzaman, M. “Modeling electric vehicle charging station expansion with an integration of renewable energy and Vehicle-to-Grid sources.” Transportation Research Part E 128, (2019): 251–279.

Ramasamy, V., Feldman, D., Desai, J., and Margolis, R. “U.S. solar photovoltaic system and energy storage cost benchmarks: Q1 2021.” National Renewable Energy Lab Technical Report: NREL/TP-7A40–80694 (NREL), Golden, CO (United States), 2021.

Said, D., Cherkaoui, S., and Khoukhi, L. “Queuing model for EVs charging at public supply stations.” Proc. 9th Int. Wireless Commun. Mobile Comput. Conf. (IWCMC), (2013): 65–70.

Sbordone, D., Bertini, I., Di Pietra, B., Falvo, M., Genovese, A., and Martirano, L. “EV fast charging stations and energy storage technologies: A real implementation in the smart micro grid paradigm.” Electric Power Systems Research 120, (2015): 96–108.

Sharma, N., Sharma, P., Irwin, D., and Shenoy, P. “Predicting solar generation from weather forecasts using machine learning.” IEEE International Conference on Smart Grid Communications (SmartGrid-Comm), 2011.

Sun, W., Neumann, F., and Harrison, G. P. “Robust scheduling of electric vehicle charging in LV distribution networks under uncertainty.” IEEE Transactions on Industry Applications 56, 5 (2020), 5785–5795.

The White House. FACT SHEET: Biden Administration Advances Electric Vehicle Charging Infrastructure. Retrieved on Nov. 15, 2021a. https://www.whitehouse.gov/briefing-room/statements-releases/2021/04/22/fact-sheet-biden-administration-advances-electric-vehicle-charging-infrastructure/.

The White House. FACT SHEET: President Biden Sets 2030 Greenhouse Gas Pollution Reduction Target Aimed at Creating Good-Paying Union Jobs and Securing U.S. Leadership on Clean Energy Technologies. Retrieved on Nov 15, 2021b. https://www.whitehouse.gov/briefing-room/statements-releases/2021/04/22/fact-sheet-president-biden-sets-2030-greenhouse-gas-pollution-reduction-target-aimed-at-creating-good-paying-union-jobs-and-securing-u-s-leadership-on-clean-energy-technologies/.

Tulpule, P. J., Marano, V., Yurkovich, S., Rizzoni, G. "Economic and environmental impacts of a PV powered workplace parking garage charging station." Applied Energy 108, (2013): 323–332.

Turitsyn, K., Sŭlc, P., Backhaus, S., and Chertkov, M. "Local control of reactive power by distributed photovoltaic generators." Proc. 1st IEEE Int. Conf. Smart Grid Communications, (2010): 79–84.

Will, C., and Schuller, A. "Understanding user acceptance factors of electric vehicle smart charging." Transportation Research Part C 71, (2016): 198–214.

Wu, D., Aliprantis, D., and Ying, L. "Load scheduling and dispatch for aggregators of plug-in electric vehicles." IEEE Transactions on Smart Grid 3, (2012): 368–376.

Yang, Y., Mao, J., Nguyen, R., Tohmeh, A., and Yeh, H.G. "Feature construction and selection for PV solar power modeling." arXiv:2202.06226, 2022.

Yudovina, E., and Michailidis, G. "Socially optimal charging strategies for electric vehicles." IEEE Transactions on Automatic Control 60, (2015): 837–842.

Zhang, T., Chen, W., Han, Z., and Cao, Z. "Charging scheduling of electric vehicles with local renewable energy under uncertain electric vehicle arrival and grid power price." IEEE Transactions on Vehicular Technology 63, 6 (2014): 2600–2612.

About the Authors

Yu Yang, PhD

Dr. Yu Yang received his BSc degree from Beijing Institute of Technology, Beijing, China, in 2004; his MSc degree from Zhejiang University, Hangzhou, China, in 2007; and his PhD from the Department of Chemical Engineering, University of Alberta, Edmonton, Canada, in 2011. He then became a postdoctoral associate at the Massachusetts Institute of Technology. He currently is an assistant professor in the Department of Chemical Engineering, California State University, Long Beach. His research interests include data-driven modeling, advanced process control, machine learning, global optimization under uncertainty, and the analysis and design of renewable energy systems.

Hen-Geul Yeh, PhD

Dr. Hen-Geul Yeh received his BSc degree in engineering science from National Chen Kung University, Taiwan, ROC, in 1978, and his MSc degree in mechanical engineering and his PhD in electrical engineering from the University of California, Irvine, in 1979 and 1982, respectively. Since 1983, he has been with the Electrical Engineering Department at CSULB and has served as the Department Chair since 2016. In addition to his technical and engineering excellence, he was selected as a NASA JPL Summer Faculty Fellow twice, in 1992 and 2003, and the Boeing Welliver Faculty Fellow in 2006. His research interests include DSP/Communication/Control algorithms development using MATLAB, and their implementation using FPGA and digital signal processors with applications in communication systems, smart grids, optimization, controls, and electrical event detection, with a focus on real-time digital signal processing, Wi-Fi and Wi-MAX, adaptive systems, and mobile communication in multipath fading channels. He has published over 100 research papers on signal processing, communications, controls, and smart grids.